Electronic structure and magnetic coupling in copper oxide superconductors

Y. J. Wang*
Department of Physics, State University of New York at Stony Brook, Stony Brook, New York 11794

M. D. Newton
Department of Chemistry, Brookhaven National Laboratory, Upton, New York 11973

J. W. Davenport
Department of Physics, Brookhaven National Laboratory, Upton, New York 11973
(Received 10 December 1991; revised manuscript received 29 July 1992)

The electronic structure and magnetic coupling in La_2CuO_4 and Nd_2CuO_4 have been analyzed using the results of all-valence-electron calculations for $(Cu_2O_{11})^{18-}$, $(Cu_4O_{12})^{16-}$, and $(Cu_4O_{20})^{32-}$ clusters, and their p- and n-doped variants, embedded in a Madelung potential to represent the crystal environment. The calculations employ the semiempirical incomplete neglect of differential overlap (INDO) method, which is parametrized on the basis of atomic and molecular spectroscopic data, but which makes use of no data from copper oxide materials. The energies of the low-lying cluster spin states are fitted to a Heisenberg Hamiltonian and yield values of J (134 meV for La_2CuO_4 and 117 meV for Nd_2CuO_4) in close agreement with experiment. The evaluation of J can be compactly represented in terms of the parameters (t, U, and V) of a one-band Hamiltonian that controls resonance among covalent and ionic valence-bond structures. The resonance mixing is achieved by configuration interaction (CI) among valence-band structures defined in terms of localized molecular orbitals (LMO's) obtained from self-consistent field (SCF) INDO calculations. P doping is found to involve strong hybridization of the $2p\sigma$ orbitals of the in-plane oxygen ions and the $3d_{x^2-y^2}$ orbitals of the Cu ions, and the resulting holes are predominantly ($\sim 60\%$) located in the $2p\sigma$ orbitals. The lowest-energy n-doped cluster states involve addition of electrons to the $4s/4p$ Cu atom manifolds. However, the separation of these states from low-spin ($3d^{10}$) alternatives is uncertain because of apparent sensitivity to the representation of the crystal potential, as found by Martin.

I. INTRODUCTION

Among the many challenges posed by the discovery of high-T_c superconductors, a correct description of the electronic structure is an indispensable first step toward unravelling the various novel properties of these materials. The standard "band structure" approach, using the local density approximation (LDA), has been extremely successful at describing many crystalline solids and also many molecules. For example, the lattice constant, cohesive energy, and magnetic moments of the $3d$ transition metals iron, cobalt, and nickel are well described by the theory. However, the theory has not worked well for the transition metal oxides such as FeO, CoO, NiO, and CuO. Since the physics of the high-T_c materials seems closely related to that of the other oxides, one should be cautious in applying the LDA. Indeed, several calculations[1-6] on La_2CuO_4 have failed to reveal the antiferromagnetism so well documented by neutron[7] and Raman scattering.[8] This is almost surely related to the "mean field" nature of the LDA and the fact that strong Coulomb interactions necessitate a more detailed treatment of electron correlation.[9]

In the solid-state literature, this has led to the widespread use of Hubbard models,[10] where the large Coulomb interaction is explicitly recognized. For high-T_c materials, the problem is often reduced to involve only the strongly hybridized Cu $3d_{x^2-y^2}$ and O $2p_{x,y}$ orbitals in the plane of the nearest-neighbor Cu—O bonds, as in the case of the three-band Hubbard model of Emery,[11-15] or further renormalized to an effective one-band model, like the resonating valence bond (RVB) model of Anderson,[16,17] or that of Hybertsen, Schlüter, and Christensen,[15] and the t-J model of Zhang and Rice.[18] Two major concerns related to model Hamiltonians are how the parameters are determined and, more importantly, how well they describe the electronic structure. Eskes, Tjeng, and Sawatzky,[19] and Eskes, Sawatzky, and Feiner (ESF)[20] included all the Cu $3d$ and O $2p$ states in their model Hamiltonian cluster calculations and derived the effective parameters by comparison with photoelectron spectroscopic data. Hybertsen, Stechel, Schlüter, and Jennison (HSSJ)[21] adopted a constrained density-functional approach and a mean-field fit to the three-band Hubbard model. Neither group included the spatially diffuse Cu $4s$ and $4p$ orbitals in its calculations. (In fact, the peak positions of the $4s$ and $4p$ wave functions are closer to O sites than to Cu sites, as discussed below.) The inclusion of them in the model would allow a better treatment of the many-body effects like screening and polarization, and would also serve to "renormalize" the hopping integrals.

The experimental Heisenberg superexchange J value for La_2CuO_4 is a stringent test for the low-energy spectrum derived from these methods. ESF's calculated J value is about two times larger than the observed one.[7,8] HSSJ's J is in good agreement with the experimental

value; however, they have emphasized that the 10% uncertainty in their parameters allows a 50% deviation in the very sensitive J result. Great sensitivity of J to the details of the computational model has also been experienced in computational studies based on the techniques of *ab initio* quantum chemistry.[22–26] In the very recent study reported by Martin,[24] the results of *ab initio* configuration interaction (CI) studies for discrete molecular clusters were employed in determining the parameters of an effective one-band Hubbard model. The relative energies of different doped states [obtained by removal (p doping) or addition of an electron (n doping)] were also discussed. The nature of the orbitals associated with doping is a topic of considerable interest in the theoretical[14,18–20,22–24,27] and experimental[28] literature.

While attractive in terms of their compact simplicity, conventional Hubbard models (e.g., the one- or three-band types) entail a high degree of renormalization, being governed by effective parameters which bear an unclear relationship to the all-electron Hamiltonian from which they were derived. In particular, it is unclear how broad the valid energetic range of a given low-order (e.g., one- or three-band) Hubbard model is. Processes of interest in the copper oxides cover a very broad energy range, from the low-energy transitions among different spin states (<1 eV) to ligand-field and charge-transfer transitions as well as ionization and electron attachment processes which involve transition energies of the order of $\sim 1-10$ eV. One obvious variable of great importance in defining effective Hubbard parameters is the degree of response of the environment in final-state relaxation effects. Clearly, the importance of such relaxation increases appreciably as one proceeds from low-energy transitions involving no charge transfer to local charge-transfer processes, and finally to net ionization or electron attachment.

In approaching the above questions, we have adopted the techniques of quantum chemistry (examples of *ab initio* applications were noted above). These techniques can be applied to finite clusters with a multiorbital description and can span the range from small U cases where Hartree-Fock calculations (and presumably also the LDA) work well, to large U where correlation effects are crucial. This is usually done by the technique of configuration interaction (CI) or mixing of Slater determinants. Nevertheless, the task of obtaining quantitatively reliable results for clusters containing transition metal atoms on the basis of *ab initio* techniques still poses major computational problems, involving both the size of the one-electron orbital basis set and the many electron basis (i.e., the number of configurations included in the CI).[29]

As an alternative to the all-electron *ab initio* quantum chemistry model, we adopt in the present study the so-called incomplete neglect of differential overlap (INDO) model.[30–38] The INDO model is based on an all-valence electron Hamiltonian (in the present case, including the full $3d$, $4s$, and $4p$ manifold of copper and the full $2s,2p$ manifold of oxygen), which is specified in terms of certain empirically based parameters and which may be implemented at the single configuration mean field or self-consistent field (SCF) level, or at the multiconfiguration CI level. Thus it is capable of a more detailed treatment of electron correlation than that provided by the "mean-field" scheme of the LDA.

The "spectroscopic" version of INDO (INDO/S) (Refs. 31, 34, and 35) which we employ below incorporates empirical input in the following manner: (1) atomic spectroscopic data, including ionization and electron attachment energies, are used in specifying all one-electron (site energies) and two-electron (including Coulomb and exchange integrals) atomic parameters; (2) molecular spectroscopic data (including that for ligand-field and charge-transfer transitions in transition metal complexes) are employed in specifying certain atomic parameters which govern the magnitude of two-center hopping integrals. In the present application, it is essential to emphasize that none of the standard INDO parameters[35] employed in the present study are based on the properties of copper oxides.

As a result of the exploitation of empirical parameterization, together with a number of additional approximations in the specification of one- and two-electron molecular integrals, it is computationally feasible to carry out INDO calculations encompassing a broad array of electronic states for clusters containing as many as ~ 25 atoms and ~ 200 electrons, as reported below. The INDO/S method has been successful in treating electronic properties of a large variety of transition metal complexes.[33,34,39,40]

In fact, INDO has been employed to study Cu-O clusters before.[39–41] However, rather than using the spectroscopic data, the authors there chose a parametrization scheme that reproduced the results of *ab initio* calculations on organometallic compounds.[42] The $3d_{x^2-y^2}$ electrons were found to be strongly correlated and to form local moments. But further quantitative investigations such as the superexchange J value were not reported there.

Various model clusters of different size, representing La_2CuO_4 and Nd_2CuO_4 and the doped counterparts, are used in the current work. Madelung potentials were included to provide a suitable crystal environment and were defined by assigning the "standard valence charges" [i.e., $+3$ for La(Nd), $+2$ for Cu, and -2 for O] to the ionic sites outside the clusters. The calculated electronic populations support this "standard valence" presumption, giving *a posteriori* justification for its use.

The primary result of the present study is the demonstration of the ability of the standard INDO Hamiltonian (with no input from copper oxide data) to yield estimates of the Heisenberg J coefficient for La_2CuO_4 and Nd_2CuO_4 in excellent agreement with experiment. These results are obtained on the basis of very compact "valence-bond" (VB) wave functions which define the parameters of an effective one-band Hubbard Hamiltonian. The calculated J values can be expressed in terms of these parameters using second-order Rayleigh-Schrödinger perturbation theory. The success of the calculations rests on the combined influence of the atomic correlation effects implicit in the INDO parameters and the molecular correlation effects incorporated via the CI (i.e., the VB resonance). The SCF results by themselves yield an in-

correct ferromagnetic picture of the ground state.

Additional calculations are reported for the properties of doped systems obtained by removing or adding an electron to the parent cuprates, and the effects on the one-band Hubbard model of final-state relaxation attending such processes are explored.

The methodology adopted in the present study is discussed in detail in Sec. II. Results are presented and discussed in Sec. III, and summarized in Sec. IV.

II. METHOD

A. The INDO Hamiltonian[30–38]

We express the Hamiltonian as

$$H=\sum_{ij} I_{ij}c_i^\dagger c_j+\frac{1}{2}\sum_{ikjl} U_{ikjl}c_i^\dagger c_k^\dagger c_l c_j \ , \tag{1}$$

where $c_i^\dagger(c_i)$ is the electron creation (annihilation) operator, which operates on an orthonormal basis set of spin orbitals $\{\chi_i\}$. If the basis is complete, then Eq. (1) is the exact Hamiltonian of the system (neglecting relativistic effects). The two-electron Coulomb integral U_{ijkl} is given by

$$\begin{aligned} U_{ikjl} &\equiv \langle \chi_i\chi_k|\chi_j\chi_l\rangle \\ &= \int \chi_i^*(\mathbf{r}_1)\chi_k^*(\mathbf{r}_2)(1/|\mathbf{r}_1-\mathbf{r}_2|)\chi_j(\mathbf{r}_1)\chi_l(\mathbf{r}_2)d\mathbf{r}_1 d\mathbf{r}_2 \ , \end{aligned} \tag{2}$$

where the variables include both space and spin. Clearly, the integral will be zero if χ_i and χ_j do not have the same spin, and likewise for χ_k and χ_l. In the following, we shall assume that spin integrations have been carried out and shall deal explicitly only with spatial integrals. Since the INDO approximations depend on the atomic centers involved in the integrals, we now adopt the notation

$$\chi_i \rightarrow \chi_\mu^A \ , \tag{3}$$

where the collective index i is replaced by a site designation (A) and a label for the μth orbital on that site (when necessary below the spin of χ_μ^A will be denoted by τ).

The INDO approach retains all one-center two-electron integrals of appreciable magnitude (see Appendix A),

$$U_{\mu\rho\nu\sigma}^A \equiv \langle \chi_\mu^A\chi_\rho^A|\chi_\nu^A\chi_\sigma^A\rangle \tag{4}$$

while the other two-electron integrals are evaluated according to the "zero-differential-overlap" (ZDO) approximation,[30]

$$\langle \chi_\mu^A\chi_\rho^C|\chi_\nu^B\chi_\sigma^D\rangle = \gamma_{\mu\rho}^{AC}\delta_{AB}\delta_{CD}\delta_{\mu\nu}\delta_{\rho\sigma} \tag{5}$$

for $A\neq C$.

The one-electron integrals, I_{ij}, consist of diagonal "site energies," ε_μ^A, which include any Madelung contributions, and off-diagonal two-center "hopping terms," $t_{\mu\nu}^{AB}$. The total INDO Hamiltonian can thus be written as

$$\begin{aligned} H=&\sum_{A\mu\tau}\varepsilon_\mu^A n_{A\mu\tau}+\sum_{\substack{A\neq B\\ \mu\nu\tau}} t_{\mu\nu}^{AB}c_{A\mu\tau}^\dagger c_{B\nu\tau} \\ &+\frac{1}{2}\sum_{\substack{A\mu\nu\\ \sigma\rho\tau\tau'}} U_{\mu\rho\nu\sigma}^A c_{A\mu\tau}^\dagger c_{A\rho\tau'}^\dagger c_{A\sigma\tau'}c_{A\nu\tau} \\ &+\frac{1}{2}\sum_{\substack{A\neq C\\ \mu\rho}} \gamma_{\mu\rho}^{AC} n_{A\mu}n_{C\rho} \ , \end{aligned} \tag{6}$$

where $n_{A\mu\tau}\equiv c_{A\mu\tau}^\dagger c_{A\mu\tau}$ is the number operator for spin orbital $\chi_{\mu\tau}^A$ and where $n_{A\mu}$ is obtained by summing $n_{A\mu\tau}$ over alpha and beta spins.

While details of the INDO parametrization are given in Appendices A and B, we note here a few essential points:

(1) The INDO method employs a minimal valence basis: $3d$, $4s$, and $4p$ for Cu and $2s,2p$ for O, in the present application to copper oxide clusters. In comparison with low-order band models which are common in the solid-state literature (e.g., the one-, three-, and 11-band Hubbard-type models, based on the CuO_2 planar unit cell),[10–21] the INDO method constitutes a 17-band model. Thus, direct comparison of the "bare" INDO parameters with those of the lower-order methods is quite difficult. However, effective INDO one-band parameters are discussed in Sec. III.

(2) In the "spectroscopic" version of INDO used in this study (INDO/S) (Refs. 31, 34, and 35) all one-center parameters are defined in terms of atomic spectroscopic information,[43] including ionization potentials (I) and electron affinities (A). In particular, the spherical component of the self-Coulomb integral for orbital χ_μ^A [i.e., the Slater $F^0(\mu\mu)$ parameter] is evaluated according to the traditional Pariser[37] approximation

$$F_A^0(\mu\mu)=I_\mu^A-A_\mu^A \tag{7}$$

(for an s orbital, $F_A^0(\mu\mu)=\gamma_{\mu\mu}^A=U_{\mu\mu\mu\mu}^A$). Equation (7) is a particular application (to gas phase atoms) of a more general approach commonly used to define (renormalized) self-Coulomb integrals (U) in extended systems.

(3) In view of the semiempirical parametrization of the INDO/S Hamiltonian, one need not in general consider explicitly the details of the nominal basis set, which is taken as orthonormal. An important exception is the evaluation of the two-center hopping integrals $t_{\mu\nu}^{AB}$, which are taken as being proportional to the overlap integrals between Slater-type orbitals (STOs) or small linear combinations thereof:[31]

$$t_{\mu\nu}^{AB}=\left[\sum_{m=0}^{l} f_{\mu\nu}^m g_{\mu\nu}^m S_{\mu\nu}^m\right]\left[\frac{\beta_\mu^A+\beta_\nu^B}{2}\right] . \tag{8}$$

The summation is over the different angular momentum components ($m=0$ to l) of the overlap integral ($S_{\mu\nu}^m$) defined with respect to the AB axis, the $f_{\mu\nu}^m$ are the projection coefficients defined by the appropriate Euler angles, and the $g_{\mu\nu}^m$ are additional empirically determined parameters (the conventional overlap integrals $S_{\mu\nu}^m$ correspond to $g_{\mu\nu}^m=1$ for all m). Each of the additional proportionality factors, β depends only on a single atom and

was determined from least-squares fitting on the basic of INDO/S calculations of various molecular spectral transitions. As noted above, no data for copper oxides were employed in the determination of the β_μ^{Cu} and β_μ^{O} parameters. The Cu parameters are based primarily on spectra for copper halide complexes, and the oxygen parameters were fitted to spectra of organic oxides.[44] This approach offers a convenient device for defining the dependence of $t_{\mu\nu}^{AB}$ on the relative geometrical configuration of orbitals χ_μ^A and χ_ν^B, and the fact that it involves the use of nonorthogonal atomic orbitals (STO's) does not alter the assumption of an orthonormal basis set when it comes to solving the INDO secular equations.

B. SCF and CI calculations

The SCF calculations were of the spin-restricted open-shell Hartree-Fock (ROHF) type, using the procedure developed by Edwards and Zerner,[45] which maintains orthogonality between closed-shell and open-shell orbitals through the use of projection operators. The SCF method yielded converged results for the lowest-energy state of each spatial symmetry type. For the undoped states (corresponding to the charge states indicated in Fig. 1), the lowest-energy SCF solution maintained the point-group symmetry of the molecular geometry (D_{2h} or D_{4h}). However, for the doped systems, symmetry-broken wave functions yielded the lowest-energy solutions ($D_{2h}\rightarrow C_{2v}$; $D_{4h}\rightarrow C_{2v}$). Although saddle-point solutions could be obtained which reflect the full symmetry, the symmetry-broken results are presented here, since they offer a convenient representation of a localized doping site.

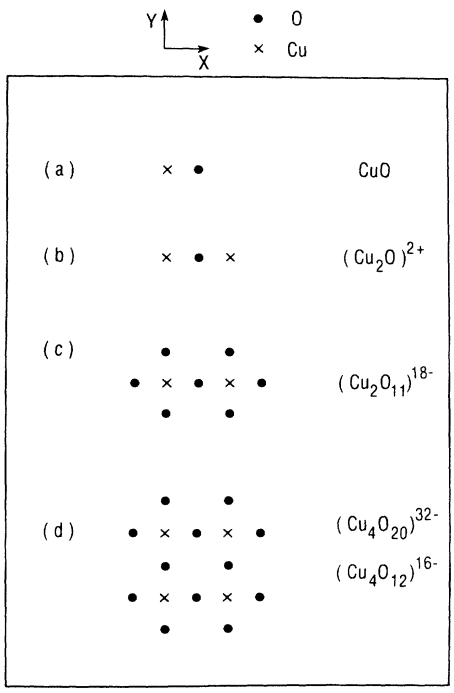

FIG. 1. The cluster models studied in this work. The indicated charges correspond to undoped species. The T-phase $(Cu_4O_{20})^{32-}$ has eight atop oxygens sitting above and below the four Cu atoms. There are no axial oxygens for the T'-phase $(Cu_4O_{12})^{-16}$. Cases (a)–(c) and (d) correspond, respectively, to the D_{2h} and D_{4h} point groups.

Convenient expressions for orbital populations (q_μ) are straightforwardly obtained by standard analysis[46] of the SCF wave functions, as discussed in Appendix C.

Although a number of exploratory CI results were carried out (employing SCF orbitals), they did not alter most of the conclusions based on SCF results which are presented below. The one place where CI was found, as expected, to be crucial, is in the evaluation of the Heisenberg parameters, J, for the undoped species.

C. Clusters

In the present work, various model clusters, illustrated in Fig. 1, are used to represent the undoped compounds La_2CuO_4 and Nd_2CuO_4, and their doped counterparts. $(Cu_2O_{11})^{18-}$ and $(Cu_4O_{20})^{32-}$ are models for La_2CuO_4, with two out-of-plane oxygens located above and below each Cu site, while $(Cu_4O_{12})^{16-}$ represents Nd_2CuO_4, where axial oxygens are absent ("plane" denotes the plane of the nearest-neighbor Cu—O bonds of the square-planar CuO_4 units). The experimental bond distances,[47,48] $r_{CuO}=1.89$ Å (in-plane) and 2.43 Å (axial) for La_2CuO_4, and $r_{CuO}=1.98$ Å (in-plane) for Nd_2CuO_4, are used in this work. The clusters are based on the tetragonal crystal structures, and the orthorhombic distortions which characterize the undoped crystalline material are not expected to have a significant effect on the properties explored in this study. The relevant Madelung energies are given in Table I.

Doping appropriately with holes or electrons brings these materials from the insulating phase into the superconducting state, and it is essential to know the atomic character of these charge carriers. The clusters involved in the study of doping are: $(Cu_2O_{11})^{x-}$, $x=17$ and 19, $(Cu_4O_{20})^{31-}$ and $(Cu_4O_{12})^{17-}$, which result from increasing or decreasing by one the electron count of the undoped clusters. In this preliminary study we only model

TABLE I. The Madelung energies for different ionic sites in the La_2CuO_4 and Nd_2CuO_4 compounds.

	Madelung energy (eV)[a]	
Ion site	La_2CuO_4[b]	Nd_2CuO_4[c]
Cu	+28.5	+24.5
O (in-plane)[d]	−21.0	−22.0
O (axial)[d]	−20.1	−20.7
La(Nd)	+27.9	+30.0

[a]That is, the energy of a point electron at the site of interest, in the field of the other ions taken as point charges ($+2|e|$ for Cu, $+3|e|$ for La and Nd, and $-2|e|$ for O), where e is the electronic charge.

[b]Based on the tetragonal crystal structure at $T=295$ K, taken from Ref. 47.

[c]Based on the tetragonal crystal structure from Ref. 48.

[d]See Fig. 1.

doping in the idealized limit of infinite dilution, since the Madelung field was maintained at the undoped value. Even though the dilute limit lies outside of the actual superconducting range [e.g., $x=0.05-0.3$ for $La_{2-x}M_xCuO_4$ (M=Sr, Ba, Ca,. . .)],[6] we nevertheless expect to obtain useful information about the nature of the charge carriers and the effect of doping on the electronic structure.

III. RESULTS AND DISCUSSION

A. Models for undoped materials

1. SCF results

Before addressing the subtle details of magnetic coupling, we examine the gross electron structural details on the basis of SCF wave functions for the various copper oxide clusters. The net negative charges on the clusters are chosen to correspond to the nominal oxidation states (Cu^{2+},O^{2-}) appropriate to the undoped materials. The lowest-energy SCF solutions are high-spin configurations with n half-filled orbitals of primarily $3d$ character (where n is the number of copper atoms in the cluster), coupled so as to yield the maximum possible spin value, $S=n/2$. As expected on the basis of crystal or ligand field theory for square planar complexes, the lowest-energy spatial configurations are those in which the open-shell $3d$-like orbitals are of $3d_{x^2-y^2}$ character (see coordinate system defined in Fig. 1). The relative energies of alternative $(Cu_2O_{11})^{18-}$ hole configurations, in which the two holes are promoted to orbitals of different $3d$ character, are presented in Table II. Since the hole-orbitals can be taken approximately as orbitals localized at each Cu atom site (see below), one might expect the two-hole excitation energies in $(Cu_2O_{11})^{18-}$ to be roughly twice those for the analogous ligand-field excitation energies at a single Cu site, and in fact such a relationship is indeed observed (see Table II) between calculated results for $(Cu_2O_{11})^{18-}$ and $(CuO_6)^{10-}$. For $(CuO_6)^{10-}$, the present INDO results and the *ab initio* CI results of Martin[24] are in reasonable agreement.

TABLE II. Relative energy of different hole configurations for undoped clusters (eV).

	INDO[b]		*Ab initio* (CI)[c]
Hole type[a]	$(Cu_2O_{11})^{18-}$	$(CuO_6)^{10-}$	$(CuO_6)^{10-}$
σ (in plane)	0.0	0.0	0.0
σ (axial)	d	2.2	1.9
π (in plane)	4.2	2.3	1.8
δ	4.5		
π (out of plane)	4.6	2.5[e]	2.3[e]

[a]Relative to the coordinate system defined in Fig. 1, the five hole types are dominated by $3d$ orbitals of type x^2-y^2, $3z^2-r^2$, xy, yz, and xz, respectively.

[b]Present INDO results based on triplet [$(Cu_2O_{11})^{18-}$] and doublet [$(CuO_6)^{10-}$] SCF calculations. As discussed in Sec. III A 1, the excited hole configurations may be viewed in terms of excitations localized at each Cu atom site. The $(Cu_2O_{11})^{18-}$ excited states, which involve two-particle excitations with respect to the ground configuration (a local excitation at each Cu site), are found (as expected) to involve excitation energies roughly twice those of the corresponding one-particle excitations in the $(CuO_6)^{10-}$ clusters.

[c]*Ab initio* results based on doublet CI calculations (Ref. 24).

[d]A converged SCF solution for the axial sigma hole state could not be obtained.

[e]Note that $3d_{xz}$ and $3d_{yz}$ are degenerate in the D_{4h} point group which governs the CuO_6 cluster.

While one may attempt to define *effective* low-order band models (see below), the hybridization of atomic orbitals reflected in the SCF MO's is quite complex. As an example, we present a one-electron density of states for $(Cu_2O_{11})^{18-}$ in Fig. 2 (based on the MO eigenvalues and the Mulliken atomic orbital populations[46] of each MO), and for reference (Fig. 3), the relative orbital energies of isolated Cu^{2+} and O^{2-} ions. The relative energies of the open-shell manifolds of the $(Cu_2O_{11})^{18-}$ and $(Cu_4O_{20})^{32-}$ clusters are displayed in Fig. 4. In each case (Figs. 2–4), the contributions of atoms not explicitly included in the cluster ion are represented by a point-charge Madelung term (see Appendix A). The Mulliken atomic orbital populations of all the undoped clusters are given in Table III, both for the total occupied manifold [Table III(A)] and the open-shell manifold which is dominated by the $3d_{x^2-y^2}$ orbitals. Further details regarding orbital hybridization in the open-shell orbitals are presented in Table IV.

The calculated Cu $3d$ populations are all reasonably close to the idealized limit, $3d^9$ [Table III(A)], consistent with inferences from experimental data.[49,50] If the Cu $4s/4p$ orbitals are considered in effect to contribute most of their populations to the region in the vicinity of the planar oxygen atoms (see comments in Appendix C), then the $\sim 3d^9$ configurations also imply a net effective atomic charge for Cu close to the value of $+2$ assumed in the specification of the Madelung potential. The exploitation of the diffuse Cu $4s$ and $4p$ orbitals by the oxide anions so as to enhance their local basis sets is not surprising, since an expansion of the oxygen charge cloud with increasing negative charge is expected. Model *ab initio* Hartree-Fock studies with very flexible basis sets show that the rms extent of the $2p$ charge cloud of O^{2-} (0.73 Å) is $\sim 50\%$ greater than for the O^{1-} anion (0.52 Å), even when the former ion is placed in a stabilizing Madelung potential equal to that appropriate for an oxide ion in the La_2CuO_4 crystal.[51]

The important role of the Madelung potential in controlling the electronic structure is underscored by model INDO studies of the CuO molecule, with bond length maintained at the crystal La_2CuO_4 value (1.89 Å).[47] As the strength of the surrounding Madelung potential is continually increased from zero (i.e., CuO *in vacuo*), the $3d$ population changes from an initial value of 9.9 to a final value of 9.0, with most of the change occurring rather abruptly as the potential varies from $\sim 30\%$ to $\sim 50\%$ of the full crystal value.

Figures 2 and 3 show that the centroid of the $2s$ and $2p$ bands is well below that of $3d$ (Figs. 2 and 3). In particular, we note that the $2p\sigma$ orbitals of the divalent in-plane oxygen atoms in the model clusters have their maximum

populations in MO's near the *bottom* of the molecular p-orbital range [e.g., the $2p_x$ orbital indicted in Fig. 2(d)], in contrast to the $2p\sigma$ orbitals of the axial oxygens [Fig. 2(e)], which lie very near the Fermi level and which have been invoked in a mechanism for superconductivity based on an excitonic model.[52] The divalent oxygens are the ones most appropriate as models for the in-plane oxide ions in the extended solid, and it is their $2p\sigma$ (and $2s$) orbitals whose hybridization with $3d_{x^2-y^2}$ orbitals is crucial for the superexchange coupling needed to establish proper energetics of spin coupling, as discussed in Sec. III A 2. In view of the significant $2s/3d$ and $2p/3d$ energy gaps (Fig. 3), orbital hybridization effects are expected to be modest, in contrast to the results of local density approximation (LDA) band structure calculations which lead to strong hybridization between $2p$ and $3d$.[1]

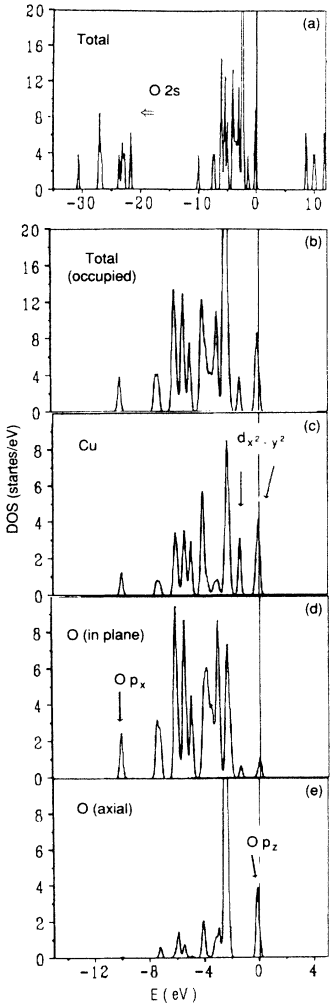

FIG. 2. Density of one-electron states (DOS) for $(Cu_2O_{11})^{18-}$. Each of the SCF orbital energies is broadened with a Gaussian function with width of 0.5 eV. The zero of energy is the Fermi level (energy of highest occupied MO): (a) total valence band; (b) total occupied manifold dominated by $2p$ and $3d$; (c) $3d$ contributions to Fig. (b) DOS; arrows identify levels dominated by $3d_{x^2-y^2}$; the $3d_{3z^2-r^2}$ contribution at the Fermi level is $\sim 35\%$ of that for the $3d_{x^2-y^2}$ orbital; (d) contributions to Fig. (b) DOS form in-plane oxygens. The arrow denotes the level dominated by the $2p\sigma$ orbital of the central (divalent) oxygen; (e) contributions to DOS of Fig. 2(b) from axial oxygens. The highest peak (arrow) is dominated by $2p\sigma$ orbitals of the axial oxygens.

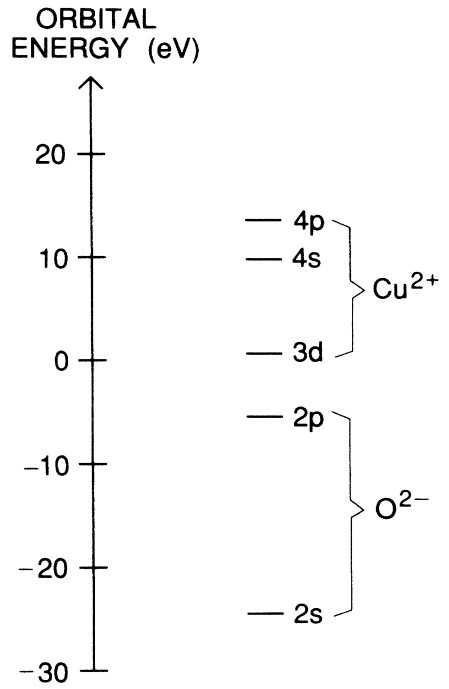

FIG. 3. Relative orbital energies (eV) of the isolated Cu^{2+} and O^{2-} ions, with inclusion of Madelung energy contributions (see Table I). The orbital energies for Cu^{2+} refer to the orbital x in the configuration $(3d)^8(x)^1$, where $x \equiv 3d_{x^2-y^2}$, $4s$, and $4p$, and $(3d)^8$ is the filled shell associated with the $3d$ orbitals of $3z^2-r^2$, xy, xz, and yz type. The O^{2-} energies are based on the $(2s)^2(2p)^6$ configuration.

In analyzing orbital hybridization, it is convenient to characterize the open-shell manifold of the undoped clus-

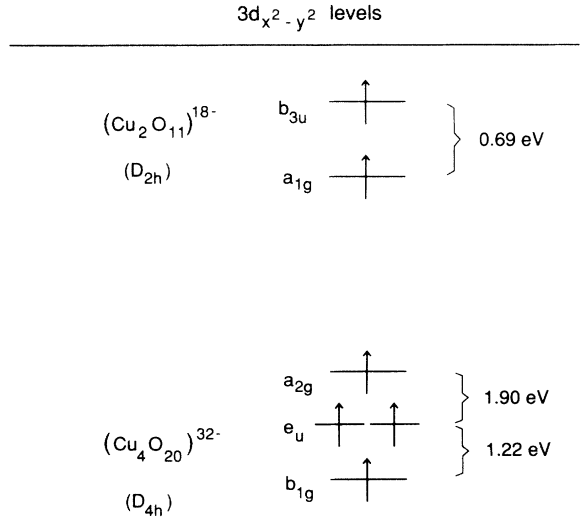

FIG. 4. Relative orbital energies (eV) for the open-shell manifolds of the clusters (i.e., involving the $3d_{x^2-y^2}$-like orbitals). Results are given for high-spin SCF wave functions [triplet and quintet, respectively, for the $(Cu_2O_{11})^{18-}$ and $(Cu_4O_{20})^{32-}$ clusters].

TABLE III. Orbital populations for undoped systems.

	Cu($3d$)	Cu($4s,4p$)	O (in plane)	O (axial)
(A) Total population[a]				
$(Cu_2O)^{+2}$	9.04	0.17	7.58	. . .
$(Cu_2O_{11})^{18-}$	8.96	2.43	7.50	7.68
$(Cu_4O_{12})^{16-}$	9.05	1.78	7.39	. . .
$(Cu_4O_{20})^{32-}$	8.64	3.14	7.32	7.63
(B) Localized hole orbital[b]				
$(Cu_2O)^{+2}$	0.71[c]	0.02	0.03	. . .
$(Cu_2O_{11})^{18-}$	0.76[c]	0.02	0.22	<0.01
$(Cu_4O_{12})^{16-}$	0.77[c]	0.02	0.20	. . .
$(Cu_4O_{20})^{32-}$	0.77[c]	0.05	0.16	0.02

[a]Mulliken populations (Ref. 46) for SCF INDO wave functions (triplet state for Cu_2 species and quintet state for Cu_4 species).

[b]Populations for the half-filled localized MO's, obtained by transformation of the canonical delocalized SCF MO's.

[c]Includes only the $3d_{x^2-y^2}$ contribution. Other $3d$ orbitals contribute <0.01 electrons, with the exception of $(Cu_2O)^{2+}$, where the $3d_{3z^2-r^2}$ orbital has a coefficient of 0.24.

ters in terms of localized MO's (LMO's), which may be defined by the unitary transformation of the canonical delocalized MO's which minimizes interorbital repulsion[53] or maximizes the separations of orbital centroids.[54] In the present case, either criterion leads to the same set of symmetry-equivalent LMO's, whose properties are summarized in Tables III(B) and IV. All four model clusters yield similar pictures of hybridization dominated by $3d_{x^2-y^2}$ and oxygen $2p\sigma$ orbitals, and aside from the $(Cu_2O)^{2+}$ clusters, where the Cu atom lacks a full planar coordination shell, all clusters yield to within $\sim 1\%$ the same fractional contribution of the $3d_{x^2-y^2}$ orbital, and lead to a picture of modest $3d_{x^2-y^2}/2p\sigma$ mixing (as anticipated above).

Table IV focuses on the orbital coefficients of the atoms involved in the linear CuOCu subunits. As noted above, these subunits are the ones which are crucial for magnetic coupling, and the similarity of the coefficients for the two different clusters is striking, even though the overall LMO populations exhibit some variation [Table III(B)]. These variations are undoubtedly artifacts of the model arising from the unavoidable presence of monovalent (i.e., "terminal") oxide atoms which have a single nearest-neighbor cation. The ratio of terminal to divalent oxide atoms is 6:1 in $(Cu_2O_{11})^{18-}$, but only 2:1 in $(Cu_4O_{20})^{32-}$.

TABLE IV. Selected atomic orbital coefficients for the localized hole orbital in the undoped species.[a]

	Atomic orbital		
Cluster	$3d_{x^2-y^2}$ (Cu)	$2s$ (O)[b]	$2p_x$ (O)[b]
$(Cu_2O_{11})^{18-}$	0.869	−0.108	−0.148
$(Cu_4O_{20})^{32-}$	0.876	−0.118	−0.136

[a]The localized orbital is as defined in footnote b, Table III.

[b]The results are given for the divalent cluster oxygen atoms (i.e., those lying between Cu atoms). These are the oxygens which are crucial for the magnetic coupling of the Cu ions. The negative signs denote anti-bonding interaction with the $3d_{x^2-y^2}$ orbital.

The LMO's may be taken as useful representations of the local spin moments on the copper ions (i.e., the local holes associated with the $\sim 3d^9$ configurations), and the dominant $3d$ character of the LMO's is consistent with the picture of the local moments inferred from experiment.[55] While the oxygen contribution to such spin moments is not directly observable for the antiferromagnetic state (where the α- and β-spin moments on oxygen would canel), we note that the relative importance of $2s$ and $2p$ implied by the ratio of LMO coefficients in the present model studies of La_2CuO_4 (0.7–0.9) is very similar to that (0.8) inferred on the basis of magnetic resonance for the magnetically active oxygen atoms which hybridize with the Cu $3d_{x^2-y^2}$ orbitals in $YBa_2Cu_3O_7$.[56] The comparable roles of $2s$ and $2p\sigma$ in hybridization of the singly filled MO's at the top of the occupied band are perhaps surprising given the particularly large energy separation of $2s$ and $3d$ orbitals (Figs. 2 and 3). However, we note that the overall hybridization of $2s$ orbitals (considering the entire occupied band) is quite small, as indicated by the fact that the $2s$ population ($\sim 1.95|e|$) departs very little from that of a closed-shell $(2s)^2$ atomic configuration. By contrast, the in-plane $2p\sigma$ populations are $\sim 1.4|e|$.

Finally we note that the general features of the electronic structure found here are very similar to those of $(CuO_6)^{10-}$ based on INDO[57] and *ab initio* results.[24]

2. *Magnetic coupling*

We now take up the task of evaluating the low-energy spectrum of states arising from the various possible spin couplings of the Cu^{2+} ions in their local $3d^9$ configurations. In previous studies of numerous transition metal complexes,[39] the INDO/S method has been shown to yield reliable values for the relative energies of different spin states. In keeping with earlier practice, we

shall represent the spin coupling information for the copper oxide clusters in terms of the exchange parameters, J, in the Heisenberg spin Hamiltonian,

$$H = \sum_{i<j} J_{ij} \mathbf{S}_i \cdot \mathbf{S}_j \ , \tag{9}$$

where the vectors **S** in the present case refer to the local spin doublets centered at each Cu site. The sign convention of Eq. (13) implies that J is positive for antiferromagnetic coupling. We also note that as defined in Eq. (9), J is the singlet/triplet splitting for two spin-$\frac{1}{2}$ particles.

The crucial role of electron correlation in evaluation of the J coefficients and the sensitivity of the calculated results to the details of the wave function have been demonstrated in a variety of prior electronic structure calculations.[20–26] Even with the semiempirical INDO method, it turns out to be essential to supplement the atomic correlation implicit in the parameters of the Hamiltonian with certain key components of molecular correlation (as in prior INDO/S studies of the energetics of different spin states[39]). Reliable and stable results for J are obtained by adopting a CI wave function which includes all possible configurations generated by excitation within the open-shell manifold. While the results are independent of particular choice of MO representation (e.g., delocalized canonical MO's or LMO's), it is convenient to employ LMO's, since this allows a pictorially appealing identification of the various "configurations" in the CI with conventional valence-bond (VB) structures, as depicted in Fig. 5. CI in the context of VB structures is generally referred to as resonance[58] [e.g., as in the resonating valence-bond (RVB) model].[16,17] Note that the B structures, while corresponding spatially to single configuration wave functions, nevertheless may involve several single determinants (the case illustrated in Fig. 5 include 1-, 2-, and 4-determinant wave functions).

The singlet VB structures employed here represent "neutral" (covalent), "ionic", and "hybrid" (i.e., mixtures of covalent and ionic) bonding types. In the higher-spin cases (triplet and quintet), one or more of the covalent electron pairs are replaced by triplet-coupled pairs. While such chemical bonding terminology may offer useful insight into the spin couping of the undoped copper oxides, it must be emphasized that the relative importance of the different VB structures depends greatly on the details of the localized MO's which serve as the effective "atomic orbitals" (AO's) of VB theory.[59–61] The LMO's employed here are clearly not pure $3d_{x^2-y^2}$ orbitals [see Tables III(B) and IV]. Nevertheless, one may still think of them as *effective* $3d_{x^2-y^2}$-like orbitals which define a one-band model. Since by construction they are orthonormal, they are closer in spirit to Wannier functions than to the non-orthogonal AO's common in traditional VB theory.[59,60]

The J_{ij} coefficients defined in Eq. (13) are obtained as follows. For each spin state, the eigenvalues of the Heisenberg Hamiltonian are matched up with the lowest energy set of eignvectors from the INDO CI defined above. Since the Heisenberg eigenvalues are linear in the J_{ij}, a linear least-squares fit of them to the INDO eigenvalues offers a convenient means of evaluating the J_{ij}. For $(Cu_2O_{11})^{18-}$ the analysis is isomorphic with the traditional hydrogen molecule problem (with the $3d_{x^2-y^2}$ *hole* providing the counterpart of the hydrogen 1*s electron* or *hole*),[24,59] and J is defined exactly by the singlet-triplet gap. For $(Cu_4O_{20})^{32-}$, six state are involved, and a nontrivial least-squares fit is necessary (e.g., see Fig. 6).

The final $J(NN)$ and $J'(NNN)$ values are listed in Table V.[62] These values, which are obtained from a model containing no parameters based on copper oxide data, are in excellent agreement with experimental estimates and imply antiferromagnetic coupling. Since the experimental analysis is based on a model which neglects nonnearest-neighbor terms in Eq. (9), our primary comparison with experiment is based on constrained least-squares fits which also neglect such terms (i.e., $J'=0$). The $(Cu_2O_{11})^{18-}$ and $(Cu_4O_{20})^{32-}$ clusters yield very similar results and suggest the absence of significant sensitivity to cluster size if the appropriate Madelung potential is used in each case. (A similar conclusion was reached in INDO cluster studies of electronic properties of crystalline LiF.[63]) The calculations also reproduce the reduction in J in proceeding from the La_2CuO_4 structure to that of Nd_2CuO_4, reflecting the effect of increased in-plane *NN* copper-oxygen separation. The calculations re-

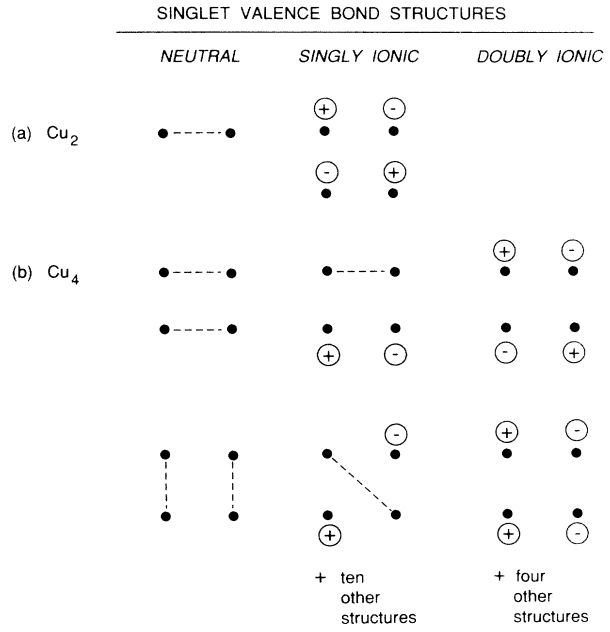

FIG. 5. Schematic depiction of valence bond structures employed in the singlet CI calculations. The dots denote Cu sites and the dashed lines indicate singlet pairing of orbitals on two different sites. Only a single orbital on each site is explicitly considered, corresponding to the $3d_{x^2-y^2}$-like orbital of the Cu atom. Empty or doubly occupied orbitals are denoted, respectively, by circles enclosing + or −. (a) For the Cu_2 cluster, one covalent and two ionic structures span the full two-electron singlet space. For triplet spin, a single structure is possible. (b) For the Cu_4 cluster the full four-electron singlet space is spanned by 2 neutral, 12 singly ionic and 6 doubly ionic structures. The triplet and quintet spaces are spanned, respectively, by 3 neutral and 12 singly ionic, and by one singly ionic structure.

veal that next-nearest-neighbor terms (J') are appreciable, and the quality of the least-squares fits is considerably less when the $J'=0$ constraint is imposed, with the σ value (see Table V) for $(Cu_4O_{20})^{32-}$ being $\sim 25\%$ of the magnitude of J [it is interesting to note that the σ values for $(Cu_4O_{20})^{32-}$ are about twice those for $(Cu_4O_{12})^{16-}$]. The near invariance of results with respect to cluster size is especially pronounced when the results of the unconstrained least-squares fit are compared [151 meV for $(Cu_2O_{11})^{18-}$ vs 144 meV for $(Cu_4O_{20})^{32-}$]. The $J'=0$ constraint, although consistent with the analysis of experimental data, is seen to introduce an artifactual increase in variation of J with cluster size. The notably poorer results yielded by the $(Cu_2O)^{2+}$ cluster suggest that full square-planar coordination of copper is necessary for a minimally acceptable model of J.

The Heisenberg Hamiltonian [Eq. (9)] is nominally defined only for nonionic states (i.e., in the present application, those for which each site has a $3d^9$ doublet configuration). However, the influence of superexchange coupling, as mediated by virtual ionic states, is implicit in the J_{ij} coefficients. In fact if the ionic structures are omitted from the CI, the resulting J_{ij} values are much reduced in magnitude [23 meV for $(Cu_2O_{11})^{18-}$ and 50 meV for $(Cu_4O_{20})^{32-}$] and their signs are *reversed;* i.e., the nonionic terms yield a weaker coupling of the ferromagnetic type. In $(Cu_4O_{20})^{32-}$ the dominant contribution is from the singly ionic structures (Fig. 5). Omission of doubly ionic terms reduces J by ~ 10 meV. The possible role of other contributions to J, beyond those obtainable from the present one-band model (e.g., virtual $2p\sigma$ to $3d_{x^2-y^2}$ excitations, can be explored by carrying out CI calculations which include excitations involving the closed-shell and empty orbital spaces. Although we have not attempted an exhaustive exploration, inclusion of large numbers of additional single excitations, relative to the VB space defined above, caused variations of no more than 10% in calculated J values. In particular, excitation of the type $2p\sigma$ to $3d_{x^2-y^2}$, which arises in Anderson's atomic orbital (AO)-based model,[64] is not found to be significant in the present CI study, which is based on an occupied orbital space consisting of variationally determined LMO's.

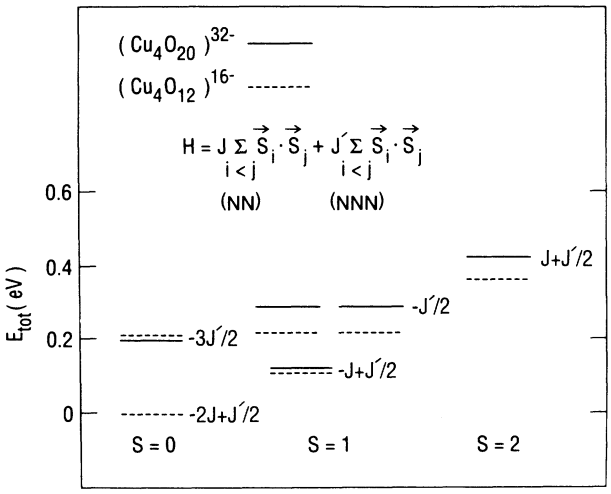

FIG. 6. Relative CI energies for various spins states of $(Cu_4O_{20})^{32-}$ (solid lines) and $(Cu_4O_{12})^{16-}$ (dashed lines). The levels are also labeled with the values they would have if they corresponded exactly to the eigenvalues of the Heisenberg Hamiltonian. The lowest energy singlet corresponds to the zero of energy for both clusters. Least-squares fittings are performed to attain the J, J' values listed in the Table V.

3. *Effective one-band model*

The evaluation of J may be compactly analyzed in terms of the parameters of an effective one-band Hamiltonian,

TABLE V. Heisenberg exchange integrals.[a]

Cluster	J_{NN} (meV)	J_{NNN} (meV)	σ (meV)[b]
La_2CuO_4($r_{CuO}=1.89$ Å)[c]			
$(Cu_2O)^{2+}$[d]	70.0	. . .	. . .
$(Cu_2O_{11})^{18-}$	151	. . .	. . .
$(Cu_4O_{20})^{32-}$	134[e] (144)	0.0(39.0)	35.0(10.3)
exp (Neutron)[f]	134	. . .	5
(Raman)[g]	128	. . .	6
Nd_2CuO_4($r_{CuO}=1.98$ Å)[c]			
$(Cu_4O_{12})^{16-}$	117[e](120)	0.0(14.4)	13.4(5.5)
exp (Raman)[g]	108	. . .	6

[a]All calculated results are obtained from full CI within the open-shell space as described in the text. J_{NN} and J_{NNN} denoted nearest-neighbor and next-nearest-neighbor interactions [see Eq. (9)].
[b]σ denotes the estimated uncertainties for the experimental values and the rms error in fitting the calculated energy levels (see Fig. 6) to the eigenvalues of the Heisenberg Hamiltonian.
[c]The crystal structures of these compounds defined the cluster geometries and Madelung potentials.
[d]This cluster is the only one which does not provide the full fourfold planar coordination for the Cu ion.
[e]Obtained from least-squares fit constraining $J'=0$, for comparison with analogously defined experimental values. The unconstrained results are in parentheses.
[f]Reference 7.
[g]Reference 8.

$$H^{\text{one band}} = t^{\text{scr}} \sum_{\substack{A<B(NN) \\ \tau}} (c^{\dagger}_{A\tau} c_{B\tau} c_{B\tau} + c^{\dagger}_{B\tau} c_{A\tau}) + \frac{U}{2} \left[\sum_{\substack{A \\ \tau \neq \tau'}} n_{A\tau} n_{A\tau'} \right] + \frac{V}{2} \left[\sum_{A \neq B(NN)} n_A n_B \right] - \frac{K}{2} \sum_{\substack{A \neq B(NN) \\ \tau, \tau'}} (c^{\dagger}_{A\tau} c^{\dagger}_{B\tau'} c_{A\tau'} c_{B\tau}) \, . \quad (10)$$

$H^{\text{one band}}$ is adapted from Eq. (6) and corresponds to the case of effective $3d_{x^2-y^2}$-type spin orbitals at each Cu atom site A, with spin (α or β) governed by the variable τ. For simplicity in Eq. (10) we have omitted the site energies ε_A [cf. Eq. (6)], which contribute only a constant energy term in the applications reported below.

We consider the $(Cu_2O_{11})^{18-}$ cluster, where only nearest-neighbor (NN) Cu-Cu interactions arise, and define the effective orbitals (A and B) as the half-filled LMO's discussed in the previous section [extension of Eq. (10) to larger systems with non-nearest-neighbor interactions is straightforward]. Direct evaluation of the parameters in $H^{\text{one band}}$, using the LMO orbital coefficients and the INDO integrals in the atomic orbital basis, yields the first column of numbers in Table VI. These are designated as "frozen orbital" values since they are defined entirely in terms of the LMO's of the undoped system, in contrast to previous approaches.[21,24]

These parameters include a screened hopping integral (t^{scr}), the self-(one-center)Coulomb integral ($U \equiv U_{AAAA}$), the NN two-center Coulomb integral ($V \equiv U_{ABAB}$), and the NN exchange integral ($K \equiv U_{ABBA}$), where reference is made to the notation introduced in Appendix B and Sec. II. The screened hopping integral t^{scr} consists of a one-electron term (t) plus a mean two-electron screening term.[65]

The NN Heisenberg superexchange coefficient J may be related to the parameters of $H^{\text{one band}}$ [Eq. (10)] through the use of second-order perturbation theory, employing the following wave functions, defined in terms of single determinants, $|i\bar{j}|$:

$$\Psi_{\text{covalent}} = (1/\sqrt{2})(|A\bar{B}| + |B\bar{A}|) \, , \quad (11a)$$

$$\Psi_{\text{ionic}} = (1/\sqrt{2})(|A\bar{A}| + |B\bar{B}|) \, , \quad (11b)$$

$$\Psi_{\text{triplet}} = (1\sqrt{2})(|A\bar{B}| - |B\bar{A}|) \, , \quad (11c)$$

TABLE VI. Effective one-band[a] parameters (eV).

Nature of[e] doped states	INDO[b] Frozen orbital	INDO[b] Relaxed	*Ab initio* (CI)[c] Relaxed[f]	Local density[d] approximation Relaxed
Nearest-neighbor				
t^{scr}	−0.59	−0.57	−0.65	−0.4
U	11.1	7.1[g]	12.8(11)	4.1
V	3.5	4.0[g,h]	2.3(2.5)	0.1−1.0
U-V	7.6	3.1[g,h]	10.5(8.5)	3.1−4.0
K	0.014	...	0.04	...
Next-nearest-neighbor				
t'^{scr}	+0.26	...	...	+0.07
V'	2.6	...	...	...

[a]Generalized one-band Hubbard model [Eq. (10)]. The signs of t^{scr} and t'^{scr} are consistent with the phase convention implied by Eq. (16).

[b]Present results based on the $(Cu_2O_{11})^{x-}$ ($x=17-19$) and $(Cu_4O_{20})^{x-}$ ($x=31-33$) clusters.

[c]Reference 24, based on $(Cu_2O_7)^{x-}$ ($x=9-11$) and $(Cu_2O_{11})^{x-}$ ($x=17-19$) clusters (Ref. 24).

[d]References 21 and 24.

[e]The parameters are defined in terms of the calculated energies for the undoped and p- and n-doped clusters. Wavefunctions for the doped states were fully relaxed except for the first column of INDO results, which are defined entirely in terms of the orbitals of the undoped state (i.e., the doped states are treated at the frozen orbital or vitual level).

[f]The values in parentheses were adjusted from the best *ab initio* CI values so as to reproduce the experimental J values (taken as ~120–130 meV) (Ref. 24).

[g]These INDO values are based on the doublet n-doped state, in which the added electron pairs up with one of the initially impaired electron. This state corresponds to the n-doped states employed in the *ab initio* (Ref. 24) and LDA (Refs. 21 and 24) results, with which comparison is made. Alternative values of U and V (respectively, 6.5 and 4.6 eV) are obtained in the n-doped species is represented by a quartet, the INDO ground state (see Sec. III B 2) in which the electron is added to an empty orbital. The U values are based on Eq. (15). The results for V are mean values obtained as $\bar{V} = [E(-2) - 2E(-1) + 2E(0) - 2E(1) + E(2)]/2$, where $E(Z)$ is the total energy of the species and Z is the net charge of the species relative to that of the undoped system ($Z=0$, ± 1, and ± 2 represents undoped, singly doped and doubly doped systems, analogous to those employed in Ref. 24).

[h]The singly doped states ($Z=\pm 1$; see footnote g) in the calculation of U and V are based on symmetry-broken SCF wave functions which yield localized doping sites. If alternatively, a delocalized representation is employed, the resulting U and V values are, respectively, 8.7 and 2.4 eV (with a doublet n-doped state) and 7.4 and 3.7 eV (with a quartet n-doped state).

where $A(\bar{A})$ and $B(\bar{B})$ denote nearest-neighbor spin orbitals with $\alpha(\beta)$ spin. We then obtain

$$J = E_{\text{triplet}} - E_{\text{singlet}} = -2K + \langle \Psi_{\text{covalent}} | H | \Psi_{\text{ionic}} \rangle^2 / (E_{\text{ionic}} - E_{\text{covalent}}) , \quad (12)$$

where

$$E_{\text{ionic}} \equiv \langle \Psi_{\text{ionic}} | H | \Psi_{\text{ionic}} \rangle$$

and

$$E_{\text{covalent}} \equiv \langle \Psi_{\text{covalent}} | H | \Psi_{\text{covalent}} \rangle ,$$

and where the $-2K$ term is the zeroth-order contribution. Equations (10) and (11) allow J to be reexpressed as

$$J = -2K + 4(t^{\text{scr}})^2/(U - V) , \quad (13)$$

where the small contribution of K to the energy denominator is neglected. With the frozen-orbital parameters displayed in Table VI, Eq. (13) yields $J = 155$ meV, in excellent agreement with the result from the variational calculations (151 meV) given in Table V.

If the one-band model [Eq. (10)] is extended to a three-band model which includes the $2p\sigma$-type LMO's, we find that the additional perturbational contributions [over and above those of Eq. (12)] amount to only a 2% change. Thus the three-band model based on LMO's containing variationally determined ligand-field mixing and hence an appreciable direct (through-space) hopping integral (t^{scr}), stands in strong contrast to the traditional three-band model based on pure $3d_{x^2-y^2}$ and $2p\sigma$ atomic orbitals, where direct coupling of Cu ion sites is negligible ($t \sim 0$). This latter model yields J as the following fourth-order expression:[11,64]

$$J = 4t_{pd}^4/\Delta_{pd}^2 U_{dd'} + 8t_{pd}^4/\Delta_{pd}^2 \Delta_{p^2dd'} , \quad (14)$$

where t_{pd} refers to NN Cu and O sites, d and d' denote $3d_{x^2-y^2}$ orbitals on NN Cu sites, and $U_{dd'}$, Δ_{pd}, and $\Delta_{p^2dd'}$ are the excitation energies, respectively, for the virtual processes, $d \rightarrow d'$, $p \rightarrow d$, and $p^2 \rightarrow dd'$ [the quantity t_{pd}^2/Δ_{pd} is the counterpart of t^{scr} in Eq. (13), and the two-center Coulomb integral ($V_{dd'}$) is neglected]. In the present INDO calculations (involving formally a 17-band model), the variational mixing embodied in the molecular orbitals is much more complex than that allowed within a perturbative three-band model. Accordingly we have not attempted to derive effective values of t_{pd}, Δ_{pd}, and $\Delta_{p^2dd'}$ from the INDO results.

The parameters t^{scr} and U may be represented in terms of ionization and electron attachment energies, yielding expressions of general applicability, including not only the present frozen-orbital (Koopmans' theorem[66]) model, but also cases involving final-state relaxation. For U we have [cf. Eq. (7)],

$$U = I - \mathcal{A} , \quad (15)$$

where I and $\mathcal{A}$ are, respectively, the local ionization energy (I) and electron attachment energy ($\mathcal{A}$). At the frozen-orbital level these are, respectively, the energy cost for *removing* an electron from the half-filled $3d_{x^2-y^2}$-type LMO in the undoped material (I) and the energy gain from *adding* an electron to the LMO ($\mathcal{A}$). Splitting of I and $\mathcal{A}$ due to delocalization of the doped states is controlled by the value of t^{scr}. Thus, for the present two-site case $[(Cu_2O_{11})^{18-}]$, t^{scr} is given by[24,67]

$$t^{\text{scr}} = \tfrac{1}{4}[(I^+ - I^-) + (\mathcal{A}^- - \mathcal{A}^+)] , \quad (16)$$

where the plus and minus signs correspond to the cases in which the ionization or electron attachment involves a symmetric (plus) or antisymmetric (minus) delocalized MO.

Values obtained from Eqs. (15) and (16) through the use of relaxed final state as well as frozen orbital final states are displayed in Table VI. The relaxed results are based on INDO SCF calculations for doped cluster states and are discussed in Secs. III C and III D. The relaxed local I and $\mathcal{A}$ values for use in Eq. (15) are obtained from broken-symmetry final-state SCF calculations which yield localized doping sites, whereas the relaxed t^{scr} values are based on $I^{\pm}$ and $\mathcal{A}^{\pm}$ values obtained from delocalized final-state SCF results.

The transfer integral t^{scr} is closely related to the transfer integrals which control the kinetics of oxidation/reduction reactions involving electron (or hole) transfer between transition metal complexes.[40] Evaluation of these latter integrals using the INDO/S method has yielded results in good agreement with available values based on model *ab initio* cluster calculations and on experiment.[40]

B. Models for doped Materials

1. p doping

As a model for the p-doped states of La_2CuO_4 we consider SCF results for the $(Cu_2O_{11})^{17-}$ cluster [similar results were found for the larger $(Cu_4O_{20})^{31-}$ cluster]. The relative energies for different final hole states are displayed in Table VII and the degree of localization and orbital character of the holes are summarized in Table VIII(A). The relative energies are in good overall agreement with the *ab initio* CI results of Martin for CuO_6^{9-} clusters,[24] indicating a ground state which places the hole primarily ($\sim 60\%$) in the $2p\sigma$-type orbitals of the planar oxygen atoms, consistent with experimental evidence.[28] In the first excited state (at ~ 1 eV), the hole is primarily concentrated in the $2p\sigma$-type orbitals of the axial oxygens. For the higher excited states, the major charge depletion is from the $3d$ orbitals.

We consider the ground p-doped state in more detail in view of the great interest in this topic reflected in the recent literature.[22–28] The overall broken-symmetry doublet state for $(Cu_2O_{11})^{17-}$ state may be characterized as a local singlet associated with the doped CuO_6 subunit and a local doublet at the other Cu ion site. The singlet CuO_6 subunit is dominated by a closed-shell configuration (as determined on the basis of various CI calculations at the INDO level), and is thus similar in character to the closed-shell model advocated by Martin,[24] in which the depletion of $2p\sigma$ population arises from strong hybridiza-

TABLE VII. Relative energies of p-doped states (eV).

Hole type	INDO[a] $(Cu_2O_{11})^{17-}$	*Ab initio* (CI) $(CuO_6)^{9-}$ [b]
σ (in-plane)	0.0	0.0
σ (axial)	0.9	1.2
δ	1.8	2.1[c]
π (out-of-plane)	1.8	
π (in-plane)	2.2	2.1
π' (in-plane)[d]	...	2.4[d]

[a]Based on spatially broken-symmetry SCF calculations, which yield localized holes (see Table VIII). For the ground (doublet) state, the doping corresponds to removal of one of the initially unpaired electrons, while for the higher (quartet) states the doping breaks an electron pair, leaving a local triplet on the doped site and a doublet one the other Cu site. The listed results are for holes dominated, respectively by $3d$ orbitals of type x^2-y^2 or $3z^2-r^2$, yz, and xz or xy.

[b]Reference 24. Analogous to the doublet and quartet states reported for $(Cu_2O_{11})^{17-}$ (see footnote a), the ground and higher states listed for $(CuO_6)^{9-}$ have, respectively, singlet and triplet spin. The holes transform like the $3d$ orbitals listed in footnote a.

[c]See footnote d of Table II.

[d]The state of 2.4 eV involves a hole dominated by in-plane oxygen $2p$ orbitals directed perpendicular to the Cu-O vectors, similar to that obtained by Guo and co-workers (Ref. 22).

tion of the $3d_{x^2-y^2}$ and $2p\sigma$ atomic orbitals in the MO's of the doped system. In the present calculation, the dominant $3d_{x^2-y^2}$ character (see Table IV) of the half-filled MO's in the initial state $[(Cu_2O_{11})^{18-}]$ is in strong contrast to the case for the fully relaxed final-state SCF wave function $[(Cu_2O_{11})^{17-}]$, where the orbital emptied as a result of the doping has only a $\sim 50\%$ contribution from $3d_{x^2-y^2}$. The strong final-state relaxation which accompanies p doping in the present study (i.e., the screening of the zeroth-order final-state $3d$ hole by $2p$ to $3d$ charge transfer) is very similar to final-state effects observed in electronic processes (ionization[34] or charge transfer[40]) involving other transition metal complexes. The INDO/S model has been shown to give a good account of such relaxation effects.[34,40]

2. *n doping*

Table VIII(B) summarizes population changes upon n doping, based on the $(Cu_2O_{11})^{19-}$ cluster. For the quartet (high spin) ground state, the n doping primarily involves the $4s/4p$ manifold, whereas for doublet (low spin) excited state (0.6 eV above the ground state), the $3d$ manifold is the most important. Previous *ab initio* calculations employing Madelung potentials have also yielded a high-spin ground state for n-doped clusters, with the dopant electron accommodated primarily by the $4s/4p$ manifold.[23,26] However, it has recently been demonstrated[24] that a more realistic crystal potential, which includes a repulsive pseudopotential for the nearby Cu^{2+} and La^{3+} ions, leads to a low-spin ground state in which the electron is added to the $3d$ manifold, thus yielding an $\sim 3d^{10}$ configuration, a result which is consistent with experiment.[28] The La^{3+} pseudo-potential apparently prevents artificial stabilization arising from the presence of very diffuse basis functions in the *ab initio* calculations. While such diffuse functions are not incorporated into the INDO model, and while the INDO model, as a result of its use of empirical atomic Coulomb and exchange in-

TABLE VIII. Charge depletion[a] in various doped states of $(Cu_2O_{11})^{18-}$.

Electron/hole type	Fraction on local CuO_6 unit[b] %	Distribution within CuO_6 unit: Cu($3d$) %	Cu($4s,4p$)[c] %	O (planar) %	O (axial) %
A p doping[d]					
σ (in plane)	82	25	−6	63	18
σ (axial)	88	41	−16	29	46
δ	86	63	−34	43	28
π (out of plane)	87	63	−33	41	29
π (in plane)	86	53	−27	50	24
B n doping[e]					
$4s$	88	−16	62	37	17
$3d_{x^2-y^2}$	58	41	5	30	24

[a]Defined in terms of loss of electronic population (based on Mulliken analysis)[46] relative to that for the undoped species $(Cu_2O_{11})^{18-}$.

[b]The broken-symmetry SCF calculations for the clusters $(Cu_2O_{11})^{x-}$, $x=17-19$) yield doped sites confined to the extent indicated on a local CuO_6 unit (based on orbital populations).

[c]The negative sign denotes a gain in $4s/4p$ electronic population upon p doping.

[d]See footnote a Table VII.

[e]$4s$ and $3d_{x^2-y^2}$ denote the orbitals experiencing the largest increase in population when the extra electron is, respectively, unpaired (quartet state) or paired (doublet state) with one of the unpaired electrons in the triplet state of the undoped SCF wave function.

[f]Denotes a loss in $3d$ population upon n doping.

tegrals, has no obvious energetic bias against a closed-shell $3d$ configuration, the relative energies of the INDO n-doped clusters may still be sensitive to the details of the crystal potential.

The n doping at the INDO level leads to a stabilization of the cluster, whereas the most recent *ab initio* energies reported by Martin for the n-doped clusters, while variational (within the constraints of symmetry-restricted wave function), are nevertheless higher than those for the undoped clusters.[24] In spite of remaining uncertainty regarding energetics, it seems clear that more detailed treatment of electron correlation would be expected to accentuate the energetic preference for the low spin (d^{10}) n-doped state.

C. Comparisons of one-band parameters

The frozen-orbital INDO parameters (i.e., based on virtual d-d' excitations) may be compared with "relaxed" parameters, based on p- and n-doped final states. It is interesting to note that the frozen-orbital INDO parameters, which give an excellent account of J, are in good overall agreement with the relaxed *ab initio* parameters of Martin, whereas the relaxed INDO value for U is closer to the relaxed value obtained from local density calculations.[21] The INDO results yield a sizable two-center Coulomb integral ($V \sim 4$ eV), both at the frozen-orbital and the relaxed level.

D. Band gap

We define the band gap as the energy required to remove an electron from the highest occupied orbital and place it in the lowest unoccupied orbital infinitely far away from the (localized) hole.[19] It is measured by the difference in threshold energies for photoemission and inverse photoemission. In a cluster it is defined as the difference between the ionization potential and the electron affinity.

$$E_{\text{gap}} = I - \mathcal{A} \ .$$

This is the same value as the U in an effective one-band model as defined in Eq. (15). From Table VI, the relaxed value of U is ~ 7 eV. The actual gap is much smaller, in the range 1.5–2.0 eV, though it is not accurately known [the threshold for photoconductivity in La_2CuO_4 is 2.0 ± 0.1 (Ref. 68)]. The reason for this discrepancy is that relaxation or polarization effects due to charge outside the cluster need to be included. These effects are difficult to estimate, but following Janssen and Nieuwpoort,[69] the polarization can be roughly found simply by considering the region outside the cluster as a dielectric with a spherical cavity. Since the dielectric constant is reasonably large, the polarization energy attending ionization or electron attachment is

$$E_{\text{pol}} \cong e^2/2R \ ,$$

where R is the effective radius of the cavity. In our case, taking $R \sim 3$ Å yields $E_{\text{pol}} \sim 2$ eV. The gap becomes

$$E_{\text{gap}} = I - \mathcal{A} - 2E_{\text{pol}} \ ,$$

where the factor -2 arises because polarization reduces I and raises $\mathcal{A}$. This gives $E_{\text{gap}} \sim 3$ eV, which is close to the observed range. Note that this correction to the gap should not be applied to calculations of the Heisenberg superexchange coupling (J) because they involve local excitations. Eskes co-workers[19] have argued that finite cluster studies are not useful in this context because of the need for this polarization correction to the gap. On the other hand, model calculations solve this problem by renomalizing the effective site energies and Coulomb interactions. Since it is our goal to study these renormalization effects by starting with bare parameters we have chosen not to do this.

IV. SUMMARY

The electronic structure and magnetic coupling in La_2CuO_4 and Nd_2CuO_4 have been analyzed using the results of all-valence-electron calculations for $(Cu_2O_{11})^{18-}$, $(Cu_4O_{12})^{16-}$, and $(Cu_4O_{20})^{32-}$ clusters, and their p- and n-doped variants, embedded in a Madelung potential to represent the crystal environment. The calculations employ the semiempirical INDO method, which is parametrized on the basis of atomic and molecular spectroscopic data, but which makes use of no data from copper oxide materials. The energies of the low-lying cluster spin-states are fitted to a Heisenberg Hamiltonian and yield values of J (134 meV for La_2CuO_4 and 117 meV for Nd_2CuO_4) in close agreement with experiment. The evaluation of J can be compactly represented in terms of the parameters (t, U, and V) of a one-band Hamiltonian which controls resonance among covalent and ionic valence-bond structures. The resonance mixing is achieved by configuration interaction (CI) among VB structures defined in terms of localized orbitals (LMO's) obtained from self-consistent field (SCF) INDO calculations.

P doping is found to involve strong hybridization of the $2p\sigma$ orbitals of the in-plane oxygen ions and the $3d_{x^2-y^2}$ orbitals of the Cu ions, and the resulting holes are predominantly ($\sim 60\%$) located in the $2p\sigma$ orbitals.

The lowest-energy n-doped cluster states involve addition of electrons to the $4s/4p$ Cu atom manifolds. However, the separation of these states from low-spin ($3d^{10}$) alternatives is uncertain, because of apparent sensitivity to the representation of the crystal potential, as found by Martin.

ACKNOWLEDGMENTS

We wish to thank Professor P. B. Allen, Professor G. A. Sawatzky, and Professor M. C. Zerner, and Dr. V. J. Emery, Dr. G. W. Fernando, Dr. R. L. Martin, Dr. J. Mei, Dr. E. Stechel, Dr. J. M. Tranquada, Dr. R. E. Watson, and Dr. M. Weinert for many useful discussions. We also thank Dr. R. L. Martin for supplying a preprint of Ref. 24 prior to publication. This work was supported by The Divisions of Chemical and Materials Sciences U.S. Department of Energy under Contract No. DE-AC02-76CH00016.

APPENDIX A

INDO parameters

We summarize here the essential details concerning the evaluation of the parameters in the INDO/S Hamiltonian [Eq. (6)].

Two-electron terms

All one-center two-electron integrals $U^A_{\mu\rho\nu\sigma}$ which can be represented as linear combinations of the empirically determined Slater-Condon factors F^k and G^k (Table IX) are retained. The other nonzero integrals are of small magnitude (hybrid integrals of the type $\langle sp|dp\rangle$) and are neglected. The spherical component of the self-Coulomb integral, $F^0(\mu\mu)$, is evaluated according to Eq. (4), while the other F^k and G^k parameters[70] listed in Table AI are obtained from atomic spectroscopic data.[43] In general, parameter values involve averaging over the various possible valence states of the atom.

The two-center Coulomb integrals, $\gamma^{AC}_{\mu\rho}$ [Eq. (4)] are evaluated according to the following empirically determined form:[34,38]

$$\gamma^{AC}_{\mu\rho}=\frac{f_\gamma e^2}{2f_\gamma e^2/[F^0_A(\mu\mu)+F^0_C(\rho\rho)]+r_{AC}}\ , \tag{A1}$$

where f_γ is set equal to 1.2 on the basis of fits to the benzene spectrum, e is the electronic charge, and r_{AC} is the interatomic separation of atomic sites A and C. Note that Eq. (A1) through its dependence on the spherical component of the self-Coulomb integrals (F^0), thereby implies a spherical averaging for the two-center γ integrals (i.e., the approximation for the $\langle\mu\rho|\mu\rho\rangle$ integral includes only the spherical component of the charge densities χ^2_μ and $\chi_{\hat\rho}{}^2$). This averaging is imposed to maintain proper rotational invariance.[34]

For sufficiently long-range interactions one expects $\gamma^{AC}_{\mu\nu}$ to approach an asymptotic limit of e^2/r_{AC} (i.e., with $f_\gamma=1.0$). In a more refined INDO model this could be achieved smoothly by incorporating an r-dependent switching function. However, for the relatively small clusters examined here, the fixed value of f_γ is probably not too severe a constraint.

TABLE IX. Slater-Condon factors (see Ref. 67) for Cu and O (eV) (see Ref. 33).

	Cu	O
$F^0(ss)=F^0(pp)$	7.68	13.00
$F^0(dd)$	13.84	...
$F^0(sd)$	9.01	...
$G^1(sp)$	2.5658	11.815
$F^2(pp)$	1.1156	6.9026
$G^2(sd)$	0.5529	
$G^1(pd)$	0.6966	
$F^2(pd)$	1.3263	
$G^3(pd)$	0.8590	
$F^2(dd)$	10.660	
$F^4(dd)$	7.1864	

One-electron terms

The on-site term, ε_μ [Eq. (6)], is given by

$$\varepsilon^A_\mu=\alpha^A_\mu-\sum_{C\neq A}Z_C\gamma^{AC}_{\mu C}+\alpha^{A,\mathrm{Mad}}_\mu\ , \tag{A2}$$

where α^A_μ includes the expectation value of the kinetic energy and the core potential on center A, the second term includes the expectation value of the core potential provided by the other centers C, with core charges Z_C, and $\alpha^{A,\mathrm{Mad}}_\mu$ is the Madelung energy (approximated as $e\phi^{A,\mathrm{Mad}}$, where $\phi^{A,\mathrm{Mad}}$ is the Madelung potential at site A). The Madelung potential[71] includes long-range interactions involving atomic sites beyond those contained in the molecular cluster and is evaluated by the Ewald method[72] on the basis of a simple point-charge Coulombic model, in contrast to the more elaborate expression employed for the shorter-range two-center interactions within the cluster [Eq. (A1)]. The differences between the values calculated here and those given in Ref. 71 are presumably related to small differences is assumed values for atomic coordinates. Variations of ±0.01 Å in Cu—O bond lengths lead to variations of $\sim\pm0.3$ eV in Madelung energies.

The α^A_μ terms [Eq. (A2)] are empirically determined in terms of atomic ionization energies, and have been assigned the following values (eV): $\alpha^{\mathrm{Cu}}_{4s}=-97.2$; $\alpha^{\mathrm{Cu}}_{4p}=-93.1$; $\alpha^{\mathrm{Cu}}_{3d}=-139.2$; $\alpha^{\mathrm{O}}_{2s}=-89.6$; and $\alpha^{\mathrm{Cu}}_{2p}=-75.3$.

The quantity $\gamma^{AC}_{\mu C}$ in Eq. (A2) is a mean two-center Coulomb integral in which the various $\gamma^{AC}_{\mu\rho}$ contributions are weighted according to the occupations of the orbitals χ^C_ρ in the ground state of atom C.[34] Through its use of a common set of Coulomb integrals in both one- [Eq. (A2)] and two-electron [Eq. (A1)] terms, the INDO parametrization maintains reasonable balance (i.e., proper screening) between attractive and repulsive energy components of the total energy.

The hopping integral $t^{AB}_{\mu\nu}$ is evaluated according to Eq. (8), using the empirically determined values (eV), $\beta^{\mathrm{Cu}}_{4s}=\beta^{\mathrm{Cu}}_{4p}=-1.0$, $\beta^{\mathrm{Cu}}_{3d}=-33.0$, $\beta^{\mathrm{O}}_{2s}=\beta^{\mathrm{O}}_{2p}=-34.0$.[35] The necessary overlap integrals depend on the Slater-type orbital (STO) exponents (ζ). The empirically determined values are as follows:[73] the minimal basis for O $2s$ and $2p$ are $2.275a_0^{-1}$, for Cu $4s$ and $4p$ they are $1.482a_0^{-1}$, while for $3d$ on Cu, a two-component STO basis is specified by exponents $2.765a_0^{-1}$ and $6.795a_0^{-1}$, together with linear coefficients 0.6968 and 0.4473, respectively. Putting these values into Eq. (8) leads to $t_{dp\sigma}=2.45$ eV and $t_{dp\pi}=-0.90$ eV for the nearest-neighbor Cu-O hopping. The often quoted hopping integral between a $d_{x^2-y^2}$ orbital on the copper and a p_x orbital on the oxygen is in fact $\sqrt{\frac{3}{2}}t_{dp\sigma}=2.12$ eV. For the oxygen-oxygen interaction we find $t_{pp\sigma}=0.58$ eV and $t_{pp\pi}=-0.04$ eV. This makes use of the factor $g_{\mu\nu}$ in Eq. (8) which are 1.267 for $t_{pp\sigma}$ and 0.64 for $t_{pp\pi}$. We note that compared to parametrizations in terms of three-band Hubbard models (see, e.g., Ref. 15) the hopping integrals in this work (which employs nominally a 17-band model) are significantly different. In particular $t_{pp\sigma}$ is smaller while $t_{dp\sigma}$ is larger.

Both of these effects are partly due to the addition of Cu 4*s* and 4*p* orbitals which significantly enhance the O-O hopping (relative to the bare $t_{pp\sigma}$ value) and, via overlap of Cu 4*s* with neighboring Cu 3*d*, reduce the Cu-O hopping (relative to the bare $t_{dp\sigma}$ value).

APPENDIX B

Screening of hopping integrals

Insight into the INDO hopping integrals $t_{\mu\nu}^{AB}$ may be gained from considering the matrix element of the Hamiltonian with respect to two single determinant wave functions, ψ_μ and ψ_ν, which differ only in the occupation numbers for a single pair of orbitals χ_μ and χ_ν (i.e., ψ_ν is related to ψ_μ by the one-electron excitation, $\chi_\mu \rightarrow \chi_\nu$):

$$\int \psi_\mu H \psi_\nu \equiv t_{\mu\nu}^{\mathrm{scr}} = t_{\mu\nu} + \sum_{k\neq\mu,\nu}^{\mathrm{occ}} (\langle \mu k | \nu k \rangle - \langle \mu k | k \nu \rangle) , \tag{B1}$$

where the sum is over all occupied spin orbitals χ_k, $k \neq \mu, \nu$. When the χ's are the atomic basis, then the ZDO approximation neglects all the two-center integrals on the right-hand side of Eq. (B1).[30] Thus the INDO empirical parametrization of $t_{\mu\nu}$ [Eq. (7)] implicitly reflects significant screening relative to the "bare" hopping integral appropriate for the atomic cores characterized by positive charges Z_C [Eq. (A2)]; i.e., the influence of the neglected two-electron terms is folded into the INDO hopping integrals.

In the more general case where the orbitals are molecular orbitals which span common atomic sites, the integrals $\langle \mu k | \nu k \rangle$ and $\langle \mu k | k \nu \rangle$, denoted respectively as two-electron hybrid and exchange integrals, will be nonzero in the INDO model, and the screening effects must be explicitly included, as discussed in Sec. III A 3. In this case, we may identify the matrix element in Eq. (B1) as an effective (screened) one-electron hopping integral, $t_{\mu\nu}^{\mathrm{scr}}$.

APPENDIX C

Orbital populations

Orbital populations (q_μ) may be defined as the diagonal elements of the first-order density matrix, ρ^{orth}, obtained from the INDO calculations, where the superscript denotes the implicit orthonormal basis in the INDO model. In practice it has generally been found more useful to define the populations in terms of the auxiliary STO basis discussed in connection with Eq. (8). The transformation from $\underline{\rho}^{\mathrm{orth}}$ to $\underline{\rho}^{\mathrm{STO}}$ is defined by the assumption that the *l* implicitly orthonormal basis (χ^{orth}) is the Löwdin-orthogonalized STO basis:[74] i.e.,

$$\chi^{\mathrm{orth}} = \chi^{\mathrm{STO}} \underline{S}^{-1/2} , \tag{C1}$$

where χ^{orth} and χ^{STO} are row vectors and $\underline{S}$ is the STO overlap matrix. In this case, the definition of orbital population must be generalized, and we adopt the Mulliken approach,[46] according to which the orbital populations are given by the diagonal elements of the matrix, $(\underline{\rho}^{\mathrm{STO}} \underline{S})$

$$q_\mu = (\underline{\rho}^{\mathrm{STO}} \underline{S})_{\mu\mu} , \tag{C2}$$

where the density matrix in the STO basis, ρ^{STO}, is given [on the basis of Eq. (C1)] by

$$\underline{\rho}^{\mathrm{STO}} = \underline{S}^{-1/2} \underline{\rho}^{\mathrm{orth}} \underline{S}^{-1/2} . \tag{C3}$$

All of the populations presented in the tables are based on single-configuration SCF wave functions, since they were found to be quite similar to those obtained from calculations including CI. In the SCF case, where $\underline{\rho} = \underline{C}\underline{C}^\dagger$ and $\underline{C}$ is the matrix of coefficients of the occupied MO's (taken as column vectors), we obtain [using Eqs. (C2) and (C3)],

$$\begin{aligned} q_\mu &= \langle (\underline{C}^{\mathrm{STO}})(\underline{C}^{\mathrm{STO}})^\dagger \underline{S} \rangle_{\mu\mu} \\ &= (\underline{S}^{-1/2} (\underline{C}^{\mathrm{orth}})(\underline{C}^{\mathrm{orth}})^\dagger \underline{S}^{1/2})_{\mu\mu} . \end{aligned} \tag{C4}$$

Since the copper 4*s* and 4*p* orbitals are spatially diffuse, with centroid $\bar{r} = 1.83$ Å vs a CuO bond length of 1.89 Å, it is probably more appropriate as a first approximation to assign their populations to the nearest-neighbor (in-plane) oxygen atoms rather than to the copper atom.

*Present address: Institute of Theoretical Physics, Chalmers University of Technology, S-412 96 Götenborg, Sweden.

[1] L. F. Mattheiss, Phys. Rev. Lett. **58**, 1028 (1987).
[2] L. F. Mattheiss and D. R. Hamann, Solid State Commun. **63**, 395 (1988).
[3] J. Yu, A. J. Freeman, and J.-H. Xu, Phys. Rev. Lett. **58**, 1035 (1987); S. Massida, J. Yu, and A. J. Freeman, Physics **C152**, 251 (1988).
[4] F. Herman, R. V. Kasowski, and W. Y. Hus, Phys. Rev. B **36**, 6904 (1987); **38**, 204 (1988); Physica C **153-155**, 629 (1988); T. C. Leung, X.-W. Wang, and B. N. Harmon, Phys. Rev. B **37**, 384 (1988).
[5] M. Weinert and G. W. Fernando, Phys. Rev. B **39**, 835 (1988).
[6] W. E. Pickett, Rev. Mod. Phys. **61**, 433 (1989).
[7] G. Aeppli *et al.*, Phys. Rev. Lett. **62**, 2052 (1989).
[8] P. E. Sulewski, P. A. Fleury, K. B. Lyons, S.-W. Cheong, and Z. Fisk, Phys. Rev. B **41**, 225 (1990).
[9] N. F. Mott, Proc. R. Soc. London, Ser. A **62**, 416 (1949).
[10] J. Hubbard, Proc. R. Soc. London, Ser. A **277**, 237 (1964).
[11] V. J. Emery, Phys. Rev. Lett. **58**, 2794 (1987); V. J. Emery and G. Reiter, Phys. Rev. B **38**, 4547 (1988).
[12] C. M. Varma, S. Schmitt-Rink, and E. Abrahams, Solid State Commun. **62**, 681 (1987).
[13] J. E. Hirsch, S. Tang, E. Loh, Jr., and D. J. Scalapino, Phys. Rev. Lett. **60**, 1668 (1988); Phys. Rev. B **39**, 243 (1989).
[14] E. B. Stechel and D. R. Jennison, Phys. Rev. B **38**, 4632 (1988).
[15] M. S. Hybertsen, M. Schlüter, and N. E. Christensen, Phys. Rev. B **39**, 9028 (1989).
[16] P. W. Anderson, Science **235**, 1196 (1987); P. W. Anderson, G. Baskaran, Z. Zou, and T. Hsu, Phys. Rev. Lett. **58**, 2790 (1987).

[17]G. Baskaran, Z. Zou, and P. W. Anderson, Solid State Commun. **63**, 973 (1987).

[18]F. C. Zhang and T. M. Rice, Phys. Rev. B **37**, 3759 (1988).

[19]H. Eskes, L. H. Tjeng, and G. A. Sawatzky, Phys. Rev. B **41**, 288 (1990); H. Eskes and G. A. Sawatzky, *ibid.* **43**, 119 (1991).

[20]H. Eskes, G. Z. Sawatzky, and L. F. Feiner, Physica C **160**, 424 (1989).

[21]M. S. Hybertsen, E. B. Stechel, M. Schlüter, and D. R. Jennison, Phys. Rev. B **41**, 11 068 (1990). The estimated range for V based on LDA calculations (which includes the value of 0.1 eV cited in Ref. 24) was communicated by E. Stechel (unpublished). The upper limit is still appreciably smaller than the values obtained from *ab initio* [24] and the present INDO cluster calculations.

[22]Y. Guo, J.-M. Langlois, and W. A. Goddard III, Science **239**, 896 (1988).

[23]R. L. Martin and P. W. Saxe, Int. J. Quantum Chem. **S22**, 237 (1988); R. L. Martin, Physica B **163**, 533 (1990).

[24]R. L. Martin, in *Cluster Models for Surface and Bulk Phenomena, NATO ASI Series,* edited by G. Pacchioni and P. S. Bagus (Plenum, New York, 1992), pp. 485–503.

[25]J. B. Grant and A. K. McMahan, Phys. Rev. Lett. **66**, 488 (1991).

[26]M. Eto and H. Kamimura, J. Phys Soc. Jpn. **60**, 2311 (1991).

[27]S. Yamamoto, K. Yamagushi, and K. Nasu, Phys. Rev. B **42**, 266 (1990); H. Kamimura and M. Eto, J. Phys. Soc. Jpn. **59**, 3053 (1990); C.-J. Mei and G. Stollhoff, Phys. Rev. B **43**, 3065 (1991).

[28]J. M. Tranquada, S. M. Heald, A. R. Moodenbaugh, and M. Suenaga, Phys. Rev. B **35**, 7187 (1987); J. M. Tranquada, S. M. Heald, A. R. Moodenbaugh, G. Liang, and M. Croft, Nature (London) **337**, 720 (1989).

[29]S. R. Langhoff and C. W. Bauschlicher, Jr., Ann. Rev. Phys. Chem. **39**, 181 (1988).

[30]J. A. Pople, D. L. Beveridge, and P. A. Dobosh, J. Chem. Phys. **47**, 2026 (1967).

[31]J. Ridley and M. Zerner, Theoret. Chim. Acta **32**, 111 (1973).

[32]G. Karlsson and M. C. Zerner, Intl. J. Quantum Chem. **7**, 35 (1973).

[33]A. D. Bacon and M. C. Zerner, Theoret. Chim. Acta (Berlin) **53**, 21 (1979).

[34]M. C. Zerner, G. H. Loew, R. F. Kirchner, and U. T. Mueller-Westerhoff, J. Am. Chem. Soc. **102**, 589 (1980).

[35]The calculations were carried out with the INDO computer code developed by M. Zerner *et al.*, University of Florida, using the standard (default) values of the parameters for transition metal complexes, as described in Appendix A. Since the focus here is on various spectroscopic states of copper oxide clusters, we have employed the "spectoscopic" version (Refs. 31 and 34) of the INDO method (INDO/S).

[36]The INDO approach exploits earlier empirical procedures for defining effective Coulomb integrals (see Refs. 37 and 38).

[37]R. Pariser, J. Chem. Phys. **21**, 568 (1953); R. Pariser and R. Parr, *ibid.* **21**, 767 (1953).

[38]N. Mataga and K. Nishimoto, Z. Phys. Chem. (Frankfurt am Main) **13**, 140 (1957).

[39]S. Larsson, K. Ståhl, and M. C. Zerner, Inorg. Chem. **25**, 3033 (1986); W. P. Anderson, W. D. Edwards, and M. C. Zerner, *ibid.* **25**, 2728 (1986); W. D. Edwards, B. Weiner, and M. C. Zerner, J. Am. Chem. Soc. **108**, 2196 (1986); J. Phys. Chem. **92**, 6188 (1988).

[40]M. D. Newton, K. Ohta, and E. Zhong, J. Phys. Chem. **95**, 2317 (1991); M. D. Newton, in *Cluster Models for Surface and Bulk Phenomenon, NATO ASI Series,* edited by G. Pacchioni and P. S. Bagus (Plenum, New York, 1992), pp. 551–563.

[41]M. C. Böhm, G. Bubeck, and A. M. Oleś, Chem. Phys. **135**, 27 (1989); G. Bubeck, A. M. Oleś, M. C. Böhm, and P. Fulde, Jpn. J. Appl. Phys. **26**, Suppl. 26-3, 2113 (1987); G. Bubeck, A. M. Oleś, and M. C. Böhm, Z. Phys. B **76**, 143 (1989).

[42]M. C. Böhm and R. Gleiter, Theoret. Chim. Acta (Berlin) **59**, 127 (1981).

[43]C. E. Moore, *Atomic Energy Levels,* Natl. Bur. Stand. (U.S.) Circ. No. 467 (U.S. G.P.O., Washington, D.C., 1999, 1952), Vol. I, Vol. II. Because of a paucity of data, some of the electron affinities are based on extrapolation of values for isoelectronic series.

[44]M. C. Zerner (private communication).

[45]W. D. Edwards and M. C. Zerner, Theor. Chim. Acta. **72**, 347 (1987).

[46]R. S. Mulliken, J. Chem. Phys. **23**, 1833 (1955).

[47]J. D. Jorgensen, H.-B. Schüttler, D. G. Hinks, D. W. Capone II, K. Zhang, M. B. Brodsky, and D. J. Scalapino, Phys. Rev. Lett. **58**, 1024 (1987).

[48]Y. Tokura, H. Takagi, and S. Uchida, Nature (London) **337**, 345 (1989); Hk. Muller-Buschbaum and W. Wollschlager, Z. Anorg. Allg. Chem. **414**, 76 (1975).

[49]J. M. Tranquada, S. M. Heald, and R. Moodenbaugh, Phys. Rev. B **36**, 5263 (1987).

[50]See also K. C. Hass, in *Solid State Physics,* edited by H. Ehrenreich and D. Turnbull (Academic, Boston, 1989), Vol. 42.

[51]M. D. Newton (unpublished).

[52]W. Weber, A. L. Shelankov, and X. Zotos, in *Mechanism of High Temperature Superconductivity,* Springer Series in Material Science, edited by H. Kamimura and A. Oshiyama (Springer-Verlag, Berlin, 1989), Vol. 11, p. 89.

[53]C. Edmiston and K. Ruedenberg, Rev. Mod. Phys. **34**, 457 (1963); J. Chem. Phys. **43**, S97 (1965).

[54]S. F. Boys, Rev. Mod. Phys. **32**, 296 (1960); S. F. Boys, in *Quantum Theory of Atoms, Molecules, and the Solid State: A Tribute to J. C. Slater* (Academic, New York, 1966), p. 253.

[55]X. L. Wang *et al.*, J. Appl. Phys. **67**, 4525 (1990).

[56]F. Mila and T. M. Rice, Physica C **157**, 561 (1989).

[57]Y. J. Wang (unpublished).

[58]L. Pauling, J. Am. Chem. Soc. **53**, 1367, 3255 (1931); **54**, 988, 3570 (1932); Proc. Natl. Acad. Sci. U.S. **18**, 293 (1932); J. Chem. Phys. **1**, 280 (1933); L. Pauling and G. W. Wheland, *ibid.* **1**, 362 (1933).

[59]See, for example, J. C. Slater, *Quantum Theory of Molecules Solids,* Vol. I (McGraw-Hill, New York, 1963), Chap. 4.

[60]J. C. Slater, J. Chem. Phys. **19**, 220 (1951).

[61]J. J. Girerd, Y. Journaux, and O. Kahn, Chem. Phys. Lett. **82**, 534 (1981).

[62]The calculated J values for the excited $3d$-hole configurations listed in Table II are all $\lesssim 5$ meV.

[63]M. Matos, B. Maffeo, and M. C. Zerner, J. Phys. C **15**, 7351 (1982).

[64]P. W. Anderson, Phys. Rev. **115**, 2 (1959).

[65]The parameter t^{scr} is evaluated according to Eq. (B1), where Ψ_μ and Ψ_ν are the INDO many-electron wave functions corresponding to the single determinants $|A\overline{B}|$ and $|B\overline{A}|$ introduced in Eq. (11). For simplicity, the occupied core electrons common to all the wave functions in Eq. (11) have been suppressed, thus defining an effective vacuum state for use with $H^{\mathrm{one-band}}$. In the context of $H^{\mathrm{one\ band}}$, the "bare" hopping component (t) of t^{scr} is the INDO one-electron contribution plus the hybrid integral contributions from the core (see Appendix B). Additional screening is provided by the

"valence" hybrid integral $h \equiv \langle AA|AB\rangle$, where A and B refer to the nearest-neighbor $3d_{x^2-y^2}$-type LMO's: $t^{\rm scr}=t+h$. The calculated value of h (0.098 eV) is comparable with that ($\sim$0.05 eV) inferred in the *ab initio* studies reported in Ref. 24. The constrained treatment of screening implicit in the Hamiltonian in Eq. (10) can be relaxed so as to accommodate more general state-specific screening effects (e.g., by replacing $t^{\rm scr}$ in $H^{\rm one\ band}$ by the "bare" hopping integral (t) and adding an explicit hybrid term to the two-electron part of $H^{\rm one\ band}$). See also Ref. 67.

[66]T. Koopmans, Physica **1**, 104 (1933).

[67]With $H^{\rm one\ band}$ [Eq. (10)], $\Delta I = I^+ - I^-$ and $\Delta A = A^+ - A^-$ are equal. If the Hamiltonian is generalized so as to include the hybrid integral $\langle dd/dd'\rangle$ explicitly (see Ref. 65), the same net result for $t^{\rm scr}$ is obtained from Eq. (16) even though ΔI and ΔA now have distinct values.[24]

[68]T. Thio, R. J. Birgeneau, A. Cassanho, and M. A. Kastner, Phys. Rev. B **42**, 10 800 (1990); see also S. Etemad, D. E. Aspnes, M. K. Kelly, R. Thompson, J.-M. Tarascon, and G. W. Hull, *ibid.* **37**, 3396 (1987); and J. Humlicek, M. Garriga, and M. Cardona, Solid State Commun. **67**, 589 (1988).

[69]G. J. M. Janssen and W. C. Nieuwpoort, Phys. Rev. B **38**, 3449 (1988); see also Ref. 24 and M. S. Islam, M. Leslie, S. M. Tomlinson, and C. R. A. Catlow, J. Phys. C **21**, L109 (1988).

[70]See, for example, J. C. Slater, *Quantum Theory of Atomic Structure* (McGraw-Hill, New York, 1963), Vol. I.

[71]J. B. Torrance and R. M. Metzger, Phys. Rev. Lett. **63**, 1515 (1989); M. S. Islam, M. Lesli, S. M. Tomlinson, and C. R. A. Catlow, J. Phys. Chem. C **21**, L109 (1988).

[72]P. P. Ewald, Ann. Phys. **64**, 253 (1921); see also J. M. Ziman, *Principle of the Theory of Solids,* 2nd ed. (Cambridge University, Cambridge, 1972), Sec. 2.3.

[73]The STO parameters are given by W. P. Anderson, W. D. Edwards, and M. C. Zerner.[39] Note that the β parameters given in this work are not the standard values[35] employed in the present work.

[74]P. O. Lowdin, J. Chem. Phys. **18**, 365 (1950).